Inorganic Chemistry
Article

Ni$_{1-x}$Pt$_x$ (*x* = 0–0.12) Hollow Spheres as Catalysts for Hydrogen Generation from Ammonia Borane

Fangyi Cheng, Hua Ma, Yueming Li, and Jun Chen*

Institute of New Energy Material Chemistry, Nankai University, Tianjin 300071, People's Republic of China

In this paper, nest-like Ni$_{1-x}$Pt$_x$ (*x* = 0, 0.03, 0.06, 0.09, and 0.12) hollow spheres of submicrometer sizes have been prepared through a template-replacement route and investigated as catalysts for generating hydrogen from ammonia borane (NH$_3$BH$_3$). Experimental investigations have demonstrated that the obtained Ni$_{1-x}$Pt$_x$ alloy hollow spheres exhibit favorable catalytic activities for both the hydrolysis and the thermolysis of NH$_3$BH$_3$. It was found that, in the presence of the Ni$_{0.88}$Pt$_{0.12}$ catalyst, the hydrolysis of NH$_3$BH$_3$ causes a quick release of H$_2$, while the thermal decomposition of NH$_3$BH$_3$ occurs at lowered temperatures with increased mass loss. The present results indicate that NH$_3$BH$_3$ along with Ni$_{1-x}$Pt$_x$ alloy hollow spheres may find some applications for small-scale on-board hydrogen storage and supply.

Introduction

Hydrogen has been considered as one of the best alternative energy carriers to satisfy the increasing demand for an efficient and clean energy supply because of its abundance, high-energy density, and environmental friendliness.[1,2] The main technical challenge for the widespread application of hydrogen is its real-time production and its safe and convenient storage.[3] As a result, various kinds of solid materials for hydrogen storage have been investigated and found to be promising.[4] Typical examples are metal/complex hydrides, metal nitrides and imides, carbon materials, inorganic nanostructures, and metal−organic frameworks.[5−11] Up to now, ammonia borane (NH$_3$BH$_3$) and related amine

borane compounds have also attracted much research interest as a candidate for hydrogen storage material.[12−20]

Although NH$_3$BH$_3$ is isoelectronic with C$_2$H$_6$, it is a solid rather than a gas at ambient temperature because of its strong polarity and intermolecular interactions that are derived from the different electronegativities of B and N atoms. As a solid material, NH$_3$BH$_3$ is stable under ambient conditions and contains a high theoretical gravimetric capacity of 19.6 wt % of hydrogen. H$_2$ can be released from NH$_3$BH$_3$ through a pyrolysis or hydrolysis route. The pyrolysis of NH$_3$BH$_3$ has

* To whom correspondence should be addressed. Fax: +86-22-2350-9118. E-mail: chenabc@nankai.edu.cn.

(1) Sperling, D.; DeLuchi, M. A. *Annu. Rev. Energy* **1989**, *14*, 375.
(2) Schlapbach, L.; Züttel, A. *Nature* **2001**, *414*, 353.
(3) Ogden, J. M. *Annu. Rev. Energy Environ.* **1999**, *24*, 227.
(4) Züttel, A. *Mater. Today* **2003**, *6*, 24.
(5) (a) Grochala, W.; Edwards, P. P. *Chem. Rev.* **2004**, *104*, 1283. (b) Holladay, J. D.; Wang, Y.; Jones, E. *Chem. Rev.* **2004**, *104*, 4767.
(6) (a) Hu, J. J.; Wu, G. T.; Liu, Y. F.; Xiong, Z. T.; Chen, P.; Murata, K.; Sakata, K.; Wolf, G. *J. Phys. Chem. B* **2006**, *110*, 14688. (b) Chen, P.; Xiong, Z. T.; Luo, J. Z.; Lin, J. Y.; Tan, K. L. *Nature* **2002**, *420*, 302.
(7) (a) Wang, J.; Ebner, A. D.; Ritter, J. A. *J. Am. Chem. Soc.* **2006**, *128*, 5949. (b) Schüth, F.; Bogdanović, B.; Felderhoff, M. *Chem. Commun.* **2004**, 2249. (c) Chen, J.; Kuriyama, N.; Xu, Q.; Takeshita, H. T.; Sakai, T. *J. Phys. Chem. B* **2001**, *105*, 11214.
(8) (a) Lim, S. H.; Luo, J.; Zhong, Z.; Ji, W.; Lin, J. *Inorg. Chem.* **2005**, *44*, 4124. (b) Chen, J.; Li, S. L.; Tao, Z. L.; Shen, Y. T.; Cui, C. X. *J. Am. Chem. Soc.* **2003**, *125*, 5284. (c) Chen, J.; Kuriyama, N.; Yuan, H. T.; Takeshita, H. T.; Sakai, T. *J. Am. Chem. Soc.* **2001**, *123*, 11813.

(9) Ströbel, R.; Garche, J.; Moseley, P. T.; Jörissen, L.; Wolf, G. *J. Power Sources* **2006**, *159*, 781.
(10) (a) Rood, J. A.; Noll, B. C.; Henderson, K. W. *Inorg. Chem.* **2006**, *45*, 5521. (b) Chen, B. L.; Ma, S. Q.; Inpata, E.; Lobkovsky, E. B.; Yang, J. *Inorg. Chem.* **2006**, *45*, 5718. (c) Rosi, N. L.; Eckert, J.; Eddaoudi, M.; Vodak, D. T.; Kim, J.; O'Keeffe, M.; Yaghi, O. M. *Science* **2003**, *300*, 1127.
(11) Seayad, A. M.; Antonelli, D. M. *Adv. Mater.* **2004**, *16*, 765.
(12) Bluhm, M. E.; Bradley, M. G.; Butterick, R.; Kusari, U.; Sneddon, L. G. *J. Am. Chem. Soc.* **2006**, *128*, 7748.
(13) Chandra, M.; Xu, Q. *J. Power Sources* **2006**, *156*, 190.
(14) Gutowska, A.; Li, L.; Shin, Y.; Wang, C. M.; Li, X. S.; Linehan, J. C.; Smith, R. S.; Kay, B. D.; Schmid, B.; Shaw, W.; Gutowski, M.; Autrey, T. *Angew. Chem., Int. Ed.* **2005**, *44*, 3578.
(15) Baitalow, F.; Baumann, J.; Wolf, G.; Jaenicke-Rößbler, K.; Leitner, G. *Thermochim. Acta* **2002**, *391*, 159.
(16) Wolf, G.; Baumann, J.; Baitalow, F.; Hoffmann, F. P. *Thermochim. Acta* **2000**, *343*, 19.
(17) Sit, V.; Geanangel, R. A.; Wendlandt, W. W. *Thermochim. Acta* **1987**, *113*, 379.
(18) Kelly, H. C.; Marriott, V. B. *Inorg. Chem.* **1979**, *18*, 2875.
(19) Ryschkewitsch, G. E.; Birnbaum, E. R. *Inorg. Chem.* **1965**, *4*, 575.
(20) Denney, M. C.; Pons, V.; Hebden, T. J.; Heinekey, D. M.; Goldberg, K. I. *J. Am. Chem. Soc.* **2006**, *128*, 12048.

been widely investigated. Experimental and computational results have revealed that ammonia borane decomposes upon melting at 385 K with a hydrogen release of approximately 6.5 wt % of the initial mass, while the H$_2$ generation is moderately exothermic with a reaction enthalpy of -21 kJ mol^{-1}.[15-17] Recently, Autrey et al. investigated the thermolysis of NH$_3$BH$_3$ within nanoporous silica, and they found that the hydrogen release properties of NH$_3$BH$_3$ were significantly enhanced because of the suppression of borazine release, the modification of decomposition enthalpy, and the lowered activation barrier.[14] With respect to the hydrolysis route, early literature has shown that NH$_3$BH$_3$ could undergo uncatalyzed solvolysis and acid-catalyzed hydrolysis with the formation of boric acid and H$_2$.[18,19] Recently, Xu and Chandra reported a high-performance hydrogen generation system based on transition metal-catalyzed hydrolysis of NH$_3$BH$_3$ at room temperature.[13]

It can be seen from previous literature[12-20] that the use of ammonia borane, especially as a source for an on-board and small-scale hydrogen supply, seems to be possible and interesting. However, two major hurdles must be overcome before its use in practical applications: (1) to develop efficient and economical catalysts for further improving the kinetic and thermodynamic properties under moderate conditions and (2) to realize the reversibility. For addressing the former target, herein we report on a new kind of catalyst, namely, nest-like Ni$_{1-x}$Pt$_x$ ($x = 0$, 0.03, 0.06, 0.09, and 0.12) submicrometer-sized hollow spheres, which exhibit favorable catalytic activities for both the hydrolysis and the thermolysis of ammonia borane. The hollow alloy spheres possess some prominent advantages over their bulk counterparts. First, the hollow structural geometry endows them with beneficial properties of low density, high surface areas, extra interior reaction space, and a savings on material, as has been shown in the case of different hollow metallic nanospheres.[21-23] Second, the porous submicrometer-sized hollow spheres that consist of firmly combined alloy nanoparticles can provide a great quantity of catalytic sites and, meanwhile, avoid the aggregation of small catalyst particles, which is a common problem facing substrate-supported metal catalysts. Furthermore, the alloying of noble metal Pt with transition metal Ni exhibits comparable catalytic activities to pure Pt and, nevertheless, greatly reduces the catalyst cost. Therefore, we suggest that the Ni$_{1-x}$Pt$_x$ hollow spheres along with NH$_3$-BH$_3$ may find possible applications in small-scale hydrogen storage and on-board supply, which are required in many hydrogen-utilization technologies such as minitype H$_2$ fuel cells.

Experimental Section

Synthesis and Characterization. All chemicals were of analytical grade and were used as purchased without further purification. The synthesis of Ni$_{1-x}$Pt$_x$ ($x = 0$, 0.03, 0.06, 0.09, and 0.12)
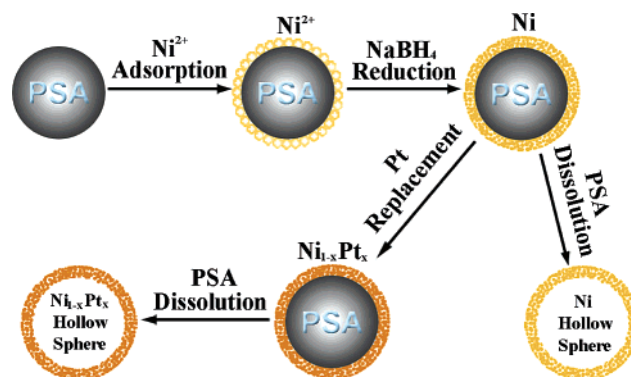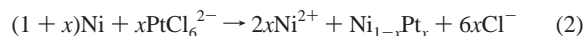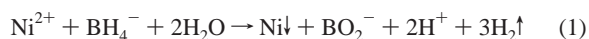

Figure 1. Illustration of the procedures for preparing Ni$_{1-x}$Pt$_x$ ($x = 0-0.12$) hollow spheres.

submicrometer-sized hollow spheres followed a PSA-assisted (PSA = poly(styrene-*co*-methacrylic acid)) template route (Figure 1), which was similar to a previous report[24] and was carried out with the following procedures. First, PSA submicrometer-sized spheres were prepared through the emulsifier-free emulsion copolymerization of styrene with methacrylic acid.[25] Second, purified PSA spheres were suspended in distilled water to form a white slurry, which was used as the template for the deposition of Ni. A mixture of the PSA slurry and a 0.4 M NiCl$_2$ aqueous solution was stirred for 30 min under argon atmosphere. Then, a freshly prepared NaBH$_4$ solution (0.012 M) was added slowly under stirring. The amount of reducing agent was over 1.5 times that of the Ni^{2+} valency to ensure a complete reduction of the metal ions to the elemental state. Afterward, a certain amount of K$_2$PtCl$_6$ (0.0012 M) was added dropwise to the above mixture according to the target molar ratio of Ni:Pt. The replacement reaction resulted in the formation of Ni$_{1-x}$Pt$_x$−PSA composite structure. Finally, the obtained core−shell composites were dispersed in toluene to completely dissolve the PSA core template. The final product was collected, washed with water and ethanol several times, dried naturally, and calcined at 350 °C for 1 h in a flowing argon gas.

The chemical reactions involved in the preparation process can be briefly expressed as

$$\text{Ni}^{2+} + \text{BH}_4^- + 2\text{H}_2\text{O} \rightarrow \text{Ni}\downarrow + \text{BO}_2^- + 2\text{H}^+ + 3\text{H}_2\uparrow \quad (1)$$

$$(1 + x)\text{Ni} + x\text{PtCl}_6^{2-} \rightarrow 2x\text{Ni}^{2+} + \text{Ni}_{1-x}\text{Pt}_x + 6x\text{Cl}^- \quad (2)$$

The phase structure of the as-synthesized samples was characterized by powder X-ray diffraction (XRD) on a Rigaku D/max 2500 X-ray diffractometer (Cu Kα radiation, $\lambda = 1.541\,78$ Å). Scanning electron microscope (SEM) images were taken on Philips XL-30 and JEOL JSM-6700F microscopes operated at the accelerating voltages of 20 and 10 kV, respectively. Transmission electron microscope (TEM) and high-resolution TEM (HRTEM) analysis were performed on a Philips Tecnai F20 microscope equipped with an energy dispersive X-ray (EDX) spectrometer using an accelerating voltage of 200 kV. Elemental composition was determined by an inductively coupled plasma (ICP) emission spectroscopy (Thermo Jarrell−Ash Corp). Specific surface areas were measured with a Micromeritics ASAP 2010 Brunauer−Emmett−Teller (BET) surface analysis instrument using nitrogen gas.

Catalyst Study. The hydrolysis of ammonia borane was carried out at controlled temperatures and concentrations. A weighed catalyst (Ni$_{1-x}$Pt$_x$ hollow spheres or commercial nickel powder)

(21) (a) Vasquez, Y.; Sra, A. K.; Schaak, R. E. *J. Am. Chem. Soc.* **2005**, *127*, 12504. (b) Liang, H. P.; Zhang, H. M.; Hu, J. S.; Guo, Y. G.; Wan, L. J.; Bai, C. L. *Angew. Chem., Int. Ed.* **2004**, *43*, 1540.
(22) Sun, Y.; Xia, Y. *Science* **2002**, *298*, 2176.
(23) Kim, S. W.; Kim, M.; Lee, W. Y.; Tyeon, T. *J. Am. Chem. Soc.* **2002**, *124*, 7642.

(24) Caruso, F.; Caruso, R. A.; Möhwald, H. *Science* **1998**, *282*, 1111.
(25) Wang, P. H.; Pan, C. Y. *Colloid Polym. Sci.* **2000**, *278*, 581.
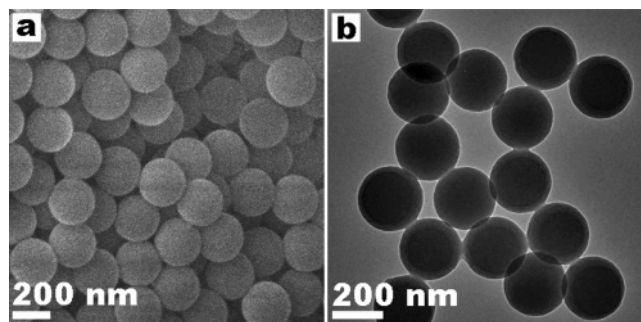
Figure 2. (a) SEM and (b) TEM images of the as-synthesized PSA submicrometer-sized spheres.

Figure 3. (A) XRD patterns of the as-synthesized (a−e) $Ni_{1-x}Pt_x$ ($x = 0$, 0.03, 0.06, 0.09, and 0.12) samples. Schematic depiction showing the (B) top view and (C) side view of the fcc crystal structure of M(111) (M = Pt or Ni).

was placed in a three-necked glass container and mixed with an aqueous NH_3BH_3 (50 mL) solution under constant stirring. The generated amount of H_2 was measured by an inverted, water-filled, and graduated burette. At different stages of the hydrolysis reaction, the resulting solutions were filtered, and the filtrates were collected for nuclear magnetic resonance (NMR) analysis. ^{11}B NMR spectra were recorded on a JEOL JNM-AL400 spectrometer with an operating frequency of 128.15 MHz. D_2O and $BF_3 \cdot (C_2H_5)_2O$ were used as a lock and an external reference, respectively. In the thermolysis experiments, $Ni_{0.88}Pt_{0.12}$ hollow spheres were added to a solution of NH_3BH_3 in methanol. This solution was then dried under vacuum to obtain a solid mixture with an approximately 1.8 wt % Pt loading. The thermal decomposition of NH_3BH_3 was monitored by a temperature-programmed desorption (TPD) system (TPD-43, BEL Japan, Inc.). In the TPD test, neat NH_3BH_3 or a mixture of NH_3BH_3 and $Ni_{0.88}Pt_{0.12}$ catalyst were investigated under a carrier gas of purified argon. The temperature was linearly increased from 25 to 250 °C at a rate of 2 °C min^{-1}. Thermogravimetry and differential thermogravimetry (TG and DTG; model TG 209, Netzsch) measurements were performed under a nitrogen atmosphere at a heating rate of 5 K min^{-1}. Fourier transform infrared (FTIR) spectra were obtained on a Bruker Tensor 27 spectrometer in the wavelength range of 400−4000 cm^{-1} on sample pellets made with KBr.

Results and Discussion

Synthesis and Characterization. $Ni_{1-x}Pt_x$ hollow spheres were synthesized through a template route by a replacement reaction, as shown in Figure 1. In our synthesis, PSA spheres were prepared and employed as sacrificial templates for the formation of hollow structures. The obtained PSA spheres are well dispersed with uniform diameters of approximately 240 nm (Figure 2). Ni is first deposited on the surface of the PSA spheres when Ni^{2+} is reduced by $NaBH_4$ (eq 1). The formation of $Ni_{1-x}Pt_x$ is attained through the replacement reaction between K_2PtCl_6 and Ni (eq 2), where the driving force comes from the large standard reduction potential gap between the Ni^{2+}/Ni (−0.250 V vs standard hydrogen electrode (SHE)) and the $PtCl_6^{-}/Pt$ (0.735 V vs SHE) redox pairs. After the partial consumption of Ni, the resultant $Ni_{1-x}Pt_x$−PSA core−shell structures are dispersed in a toluene solution to dissolve the PSA template cores, resulting in the formation of $Ni_{1-x}Pt_x$ hollow spheres.

Figure 3a shows the XRD patterns of the obtained $Ni_{1-x}Pt_x$ ($x = 0$, 0.03, 0.06, 0.09, and 0.12) samples after heating them at 350 °C for 1 h under an argon atmosphere. Three characteristic peaks of the as-synthesized nickel hollow
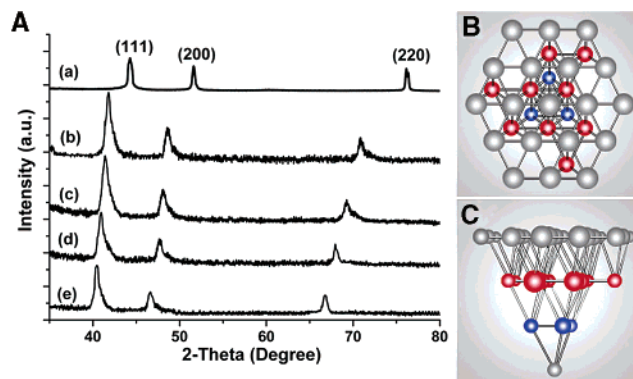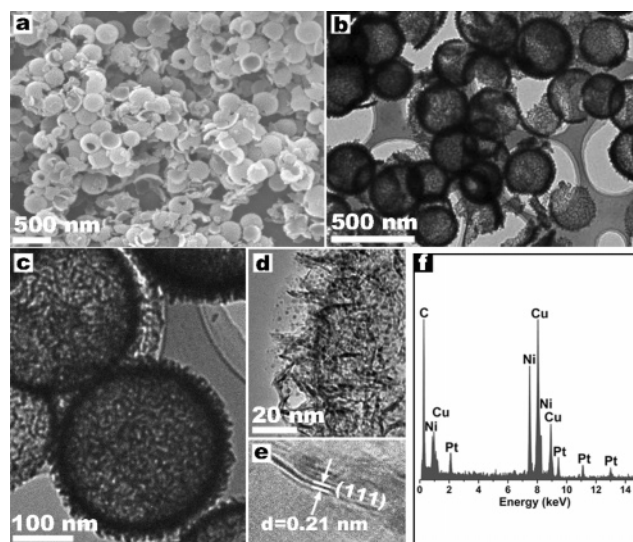
Figure 4. Morphology and composition analysis of the as-synthesized $Ni_{0.88}Pt_{0.12}$ hollow spheres: (a) typical SEM image, (b, c, d) TEM images at different magnifications, and the corresponding (e) HRTEM image and (f) EDX spectrum.

sphere can be well indexed to (111), (200), and (220) crystal planes of the face-centered cubic Ni (fcc Ni; JCPDS No. 04−0850). All of the $Ni_{1-x}Pt_x$ samples exhibit similar diffraction patterns to that of pure nickel without any extra super-lattice reflection, indicating the formation of a metallic alloy. The replacement of Pt does not change the Ni-type fcc structure (Figure 3b,c) in which Pt and Ni atoms are distributed homogeneously and randomly at the Ni position. In addition, the $d(111)$ values calculated from 2θ data are 0.204, 0.216, 0.218, 0.220, and 0.225 nm for Ni, $Ni_{0.97}Pt_{0.03}$, $Ni_{0.94}Pt_{0.06}$, $Ni_{0.91}Pt_{0.09}$, and $Ni_{0.88}Pt_{0.12}$ samples, respectively. The diffraction peaks of all the $Ni_{1-x}Pt_x$ samples shift to lower angles compared to that of the pure Ni sample, demonstrating a lattice expanding due to the substitution of the larger Pt atoms for the smaller Ni atoms.

The morphology and composition of the obtained product were investigated by SEM, TEM, EDX, and ICP analyses. Figure 4a,b show the typical SEM and TEM images of the obtained $Ni_{0.88}Pt_{0.12}$ sample. Analogous morphologies are observed for the as-synthesized $Ni_{1-x}Pt_x$ ($x = 0.03$, 0.06, and 0.09) samples (see Figure S1 in Supporting Information).

The notable different morphologies between Figure 2 and Figure 4 confirm that hollow spheres are produced by dissolving the polystyrene (PS) templates. Both complete and broken hollow spheres are obtained. The break of some hollow spheres may be caused by the removal of PS cores and/or the dispersion treatment of the samples before SEM and TEM measurements. The hollow spherical structure is almost stable at temperatures lower than 350 °C; however, more broken spheres can be found after heating the sample at 400 °C for a longer time than 2 h. High-magnification TEM images (Figure 4c,d) reveal that the wall thickness of the hollow sphere is 20−40 nm and the porous shell consists of smaller nanoparticles and nanowhiskers. These characteristics endow the Ni$_{1-x}$Pt$_x$ hollow spheres with high surface areas. The corresponding HRTEM image (Figure 4e) of a single nanowhisker displays an interlayer distance of 0.21 nm, which can be attributed to the separation between the neighboring [111] planes of Ni$_{0.88}$Pt$_{0.12}$.

EDX data (Figure 4f) of many hollow spheres prove an average elemental composition of Ni$_{0.88}$Pt$_{0.12}$; the presence of C and Cu is derived from the copper mesh and carbon film that support the sample during TEM measurement. It has been reported that the reaction of borohydride reduction of metal ions is quite complex and the product characteristic depends on the experimental conditions and procedures.[26] This reaction may yield metals,[21,26c] metal borides,[26d] or a mixture of them[26b] by varying reaction parameters such as temperature, adding rate of reactants, and gas atmosphere. Since boron cannot be detected by EDX measurement, ICP elemental analysis of the synthesized samples has been performed for further determining their composition. The boron content of the bulk sample is about 0.5 wt %, and the molar ratio of Ni and Pt determined by the ICP analysis is consistent with the EDX result. For the sake of conciseness, we intend to omit B in the present Ni$_{1-x}$Pt$_x$ catalysts though the small amount of B may partially contribute to catalytic activity.

Catalyst Study. NH$_3$BH$_3$ is stable in air and aqueous solution under ambient conditions in the absence of a catalyst, without observed H$_2$ release. We have investigated the catalytic activities of the synthesized Ni$_{1-x}$Pt$_x$ ($x = 0$, 0.03, 0.06, 0.09, and 0.12) hollow spheres for hydrogen generation by employing them as catalysts for the hydrolysis and thermolysis of NH$_3$BH$_3$. At first, the catalytic activities of commercial nickel powders (SEM image shown in Figure S2, Supporting Information) and the obtained hollow spheres have been tested and compared, with respect to the hydrolysis of aqueous NH$_3$BH$_3$ solution. Figure 5 plots the H$_2$ amount generated as a function of time for a 50 mL NH$_3$BH$_3$ solution with ∼12 mg of catalysts. Commercial nickel powders exhibit almost no catalytic activity in the hydrolysis of NH$_3$BH$_3$ at room temperature, while the synthesized nickel hollow spheres can accelerate the reaction to some extent.
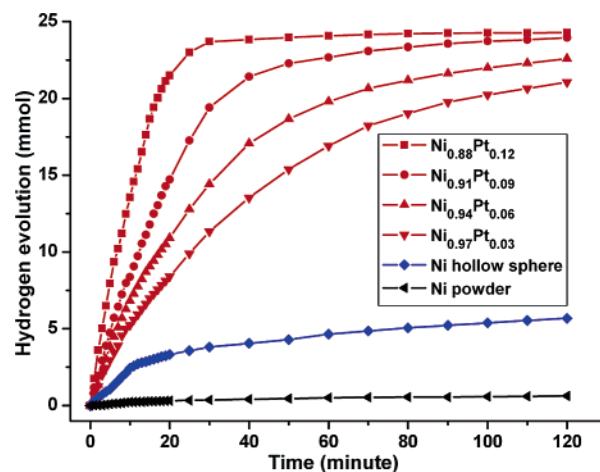
(26) (a) Ganem, B.; Osby, J. O. *Chem. Rev.* **1986**, *86*, 763. (b) Glavee, G. N.; Klabunde, K. J.; Sorensen, C. M.; Hadjipanayis, G. C. *Inorg. Chem.* **1993**, *32*, 474. (c) Park, K.; Choi, J.; Kwon, B.; Lee, S.; Sung, Y.; Ha, H.; Hong, S.; Kim, H.; Wieckowski, A. *J. Phys. Chem. B* **2002**, *106*, 1869. (d) Dong, H.; Yang, H.; Ai, X.; Cha, C. *Int. J. Hydrogen Energy* **2003**, *28*, 1095.


Figure 5. Hydrogen generation from the hydrolysis of aqueous NH$_3$BH$_3$ solution (50 mL, 0.5 wt %) containing various kinds of catalysts (12 mg) at 20 °C.

In comparison, the release of hydrogen is greatly quickened in the presence of Ni$_{1-x}$Pt$_x$ ($x = 0.03$, 0.06, 0.09, and 0.12) hollow spheres, denoting their favorable catalytic activities. The as-synthesized Ni$_{0.88}$Pt$_{0.12}$ hollow spheres are most catalytically active, with which the hydrolysis reaction of NH$_3$BH$_3$ is completed in approximately 30 min. After the completion of hydrogen release, the molar ratio of generated H$_2$ to the initial NH$_3$BH$_3$ is close to 3.0, which corresponds to approximately 8.9 wt % of the reactants (i.e., NH$_3$BH$_3$ and H$_2$O, excluding solvent water).

The catalytic performance of the as-synthesized Ni$_{0.88}$Pt$_{0.12}$ hollow spheres is comparable to that of the reported Pt black in regard to hydrogen yield.[13] However, the present catalyst is superior to pure Pt with a higher H$_2$ release rate in terms of the same Pt loading. Considering the different price between Pt and Ni, the alloy catalysts are more cost-effective. Moreover, although the hydrolysis of NH$_3$BH$_3$ can also be catalyzed by acid,[18] the related H$_2$ release rate is relatively low and depends intensively on the concentration of acid, which may cause unfavorable drawbacks in a practical application. In contrast, the present Ni$_{0.88}$Pt$_{0.12}$ can be effectively used in an NH$_3$BH$_3$ aqueous solution (pH > 7), since the hydrolysis reaction can be started by adding the solid catalyst into the solution and ceased by separating them. Furthermore, the as-synthesized alloy hollow sphere catalysts, treated by filtrating and washing, can be repeatedly utilized with no significant catalytic deactivation in the hydrolysis experiment.

The rates of hydrogen generation at different temperatures are measured in the presence of Ni$_{1-x}$Pt$_x$ hollow spheres (see an example in Figure S3, Supporting Information). Through the Arrhenius treatment of the temperature-dependent reaction rates, the activation energy of the hydrolysis of NH$_3$BH$_3$ is determined to be 70, 57, 46, 36, and 30 kJ mol^{-1} for Ni, Ni$_{0.97}$Pt$_{0.03}$, Ni$_{0.94}$Pt$_{0.06}$, Ni$_{0.91}$Pt$_{0.09}$, and Ni$_{0.88}$Pt$_{0.12}$, respectively. The order of the activation energy of Ni$_{1-x}$Pt$_x$ alloy catalysts is consistent with that of their catalytic activities. Hence, a noble element plays the key role in catalyzing the hydrolysis of ammonia borane. In addition, we have also investigated the concentration dependence of
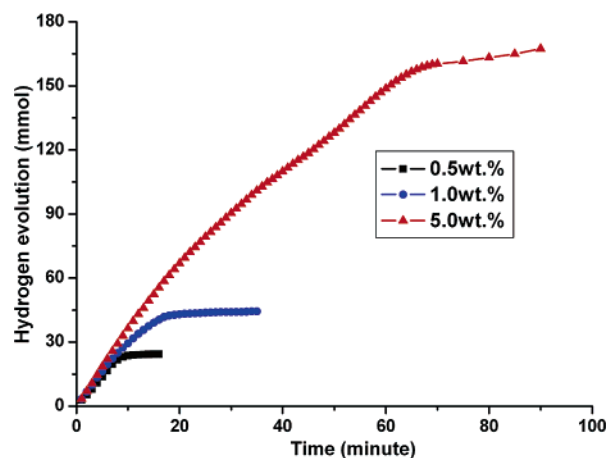
Figure 6. Hydrogen release from aqueous NH_3BH_3 solution (50 mL) with different concentrations in the presence of 20 mg of $Ni_{0.88}Pt_{0.12}$ hollow spheres.

Figure 7. ^{11}B NMR spectra of the aqueous solution measured at different stages of the hydrolysis reaction: (a) freshly prepared NH_3BH_3 (0.5 wt %) solution; after reaction for (b) 5 min and (c) 10 min in the presence of $Ni_{0.88}Pt_{0.12}$ hollow spheres; and (d) after the completion of the reaction.

the hydrolysis reaction of an aqueous NH_3BH_3 solution containing $Ni_{0.88}Pt_{0.12}$ hollow spheres. As shown in Figure 6, the concentration of NH_3BH_3 has some slight influence on the rate of hydrogen generation. The amount of H_2 generated by $Ni_{0.88}Pt_{0.12}$ hollow spheres increases nearly linearly with time before the hydrolysis reaction approaches its end, indicating an example of quasi zero-order kinetics. Hence, the synthesized $Ni_{0.88}Pt_{0.12}$ hollow spheres preserve their catalytic activities even at a solution concentration of 5 wt %. The H_2 release rate slows down during the last period of the hydrolysis process when using a more concentrated NH_3BH_3 solution. This rate drop may be due to the blocking of catalyst sites by the formed boracic precipitate. It should also be noted that the dissolution of solid NH_3BH_3 at room temperature becomes difficult at concentrations higher than 5 wt %, which happens to be a hurdle in attaining a further higher gravimetric density of H_2 production. On the other hand, there is still much room left to further improve the performance of hydrogen generation by optimizing the related experimental parameters.

NMR analysis has been carried out to study the hydrolysis process of ammonia borane. Figure 7 shows the ^{11}B NMR spectra of the resultant solutions taken at different stages of the reaction that is catalyzed by $Ni_{0.88}Pt_{0.12}$ hollow spheres. The newly prepared NH_3BH_3 solution is colorless with weak alkalinity and presents quadruplet peaks centered at $\delta = -23.9$ ppm (Figure 7a), in agreement with previous literature.[27,28] After reaction for 5 min, the relative intensities of the quadruplet peaks (Figure 7b) become lower, and a notable single ^{11}B peak is observed at $\delta = 13.1$ ppm, indicating the break of B−N and B−H bonds in NH_3BH_3 and the formation of a B−O bond. After hydrolysis for 10 min, the intensities of the ^{11}B quadruplet peaks further decrease, and the downfield peak shifts to a higher position of 10.5 ppm (Figure 7c). After the completion of the reaction, the single ^{11}B peak shifts to 6.8 ppm, and the initial resonance signals centered at -23.9 ppm disappear (Figure 7d), revealing complete consumption of NH_3BH_3. Moreover, the four
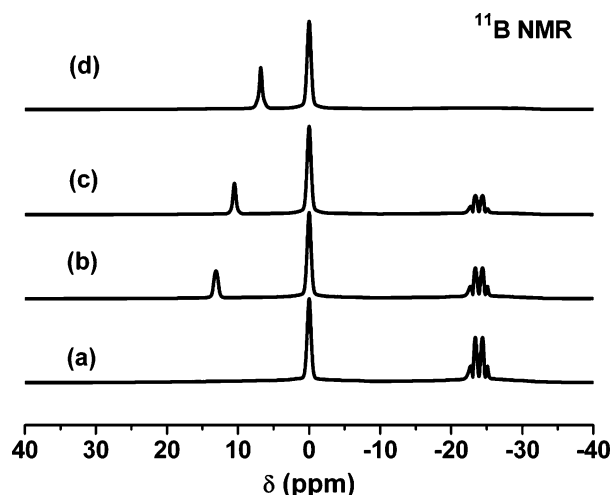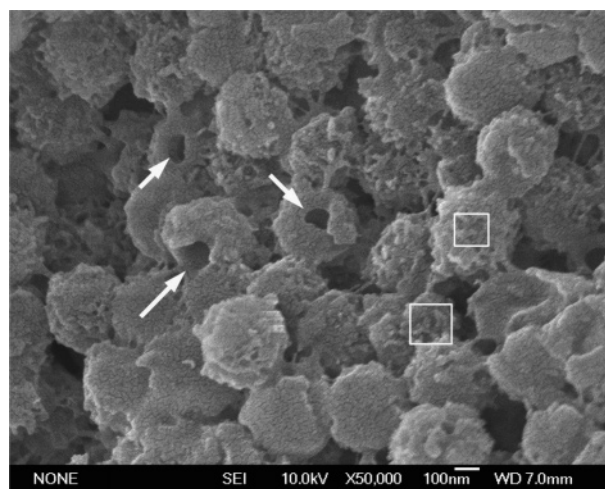
(27) Gaines, D. F.; Schaeffer, R. *J. Am. Chem. Soc.* **1964**, *86*, 1505.
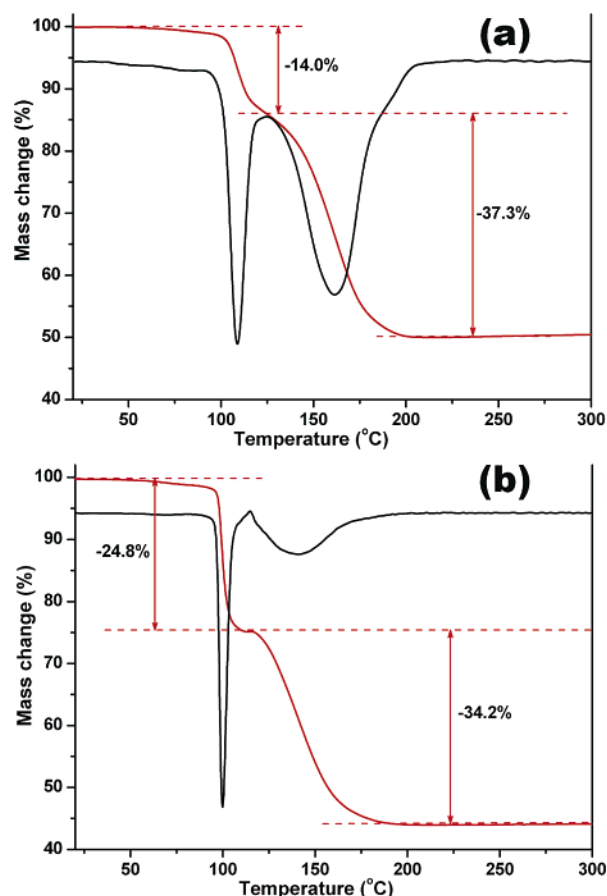(28) Heitsch, C. W. *Inorg. Chem.* **1965**, *4*, 1019.

Figure 8. SEM image of the mixture of NH_3BH_3 and $Ni_{0.88}Pt_{0.12}$ hollow spheres.

solutions analyzed exhibit pH values of 9.0, 9.4, 9.7, and 10.0, respectively. The changes of single ^{11}B resonance and pH values are possibly attributed to an equilibrium process and a rapid change between boracic compounds such as BO_2^{2-}, H_3BO_3, and other borate species.[13] Given BO_2^{2-} as the representative boracic product, the hydrolysis reaction of the NH_3BH_3 aqueous solution containing $Ni_{1-x}Pt_x$ hollow spheres can simply be described as follows:

$$NH_3BH_3 + 2H_2O \rightarrow NH_4^+ + BO_2^- + 3H_2\uparrow \qquad (3)$$
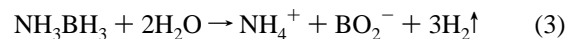
Since $Ni_{0.88}Pt_{0.12}$ hollow spheres exhibit the highest activities among the as-prepared $Ni_{1-x}Pt_x$ ($x = 0, 0.03, 0.06, 0.09,$ and 0.12) catalysts in the hydrolysis experiment, we further evaluate their catalytic performance in the thermolysis of ammonia borane. Figure 8 shows the SEM image of the mixture of NH_3BH_3 and $Ni_{0.88}Pt_{0.12}$ hollow spheres (1.8 wt % Pt loading). The white arrows mark some of the preserved hollow interiors while the white squares indicate the coating of NH_3BH_3 on the sphere surface. It can be seen from this figure that solid NH_3BH_3 and catalysts are well mixed with

Figure 9. TG (red line) and DTG (black line) curves of the thermal deposition of (a) neat NH$_3$BH$_3$ and (b) the mixture of NH$_3$BH$_3$ and Ni$_{0.88}$Pt$_{0.12}$ hollow spheres.

Figure 10. FTIR spectra of (a) unheated NH$_3$BH$_3$ and the samples obtained after heating (b) neat NH$_3$BH$_3$ and (c) NH$_3$BH$_3$ mixed with Ni$_{0.88}$Pt$_{0.12}$ at 120 °C for 2 h under nitrogen atmosphere.

sufficient contact. By repeatedly impregnating a saturated methanolic solution, NH$_3$BH$_3$ can be engaged with Ni$_{0.88}$Pt$_{0.12}$ hollow spheres with a relatively low catalyst loading. This may offer some advantages relative to the reported system of SBA-15 and NH$_3$BH$_3$, where NH$_3$BH$_3$ should be loaded into the tiny channels/pores of the nanostructured silica scaffold.[14] Furthermore, the mixture is facile to be separated by dispersing it in alcohol to collect the undissolved Ni$_{0.88}$Pt$_{0.12}$ solid; thus, the catalysts can be recovered and repeatedly used.

We have performed TG, TPD (Figure S4, Supporting Information), XRD (Figure S5, Supporting Information), and FTIR measurements to study the catalyzed thermolysis of NH$_3$BH$_3$. Figure 9 shows the TG and DTG curves of the thermal decomposition of NH$_3$BH$_3$ with and without Ni$_{0.88}$Pt$_{0.12}$ hollow spheres at the same heating rate. The neat NH$_3$BH$_3$ sample delivers two distinguished steps of mass loss, centered at 109 and 160 °C, respectively. The first step ends at 127 °C with a mass loss of approximately 14%, which probably corresponds to a hydrogen release of 2.2 mol H$_2$/mol NH$_3$BH$_3$ with the formation of nonvolatile polymeric aminoborane. Since the total mass loss exceeds the theoretical hydrogen content of NH$_3$BH$_3$ (∼19.6 wt %), it is obvious that the second step of NH$_3$BH$_3$ decomposition generates some other volatile products in addition to H$_2$, which may include gaseous BNH$_x$ species, diborane, and borazine.[15] With Ni$_{0.88}$Pt$_{0.12}$ catalysts, a large mass loss of 24.8% is

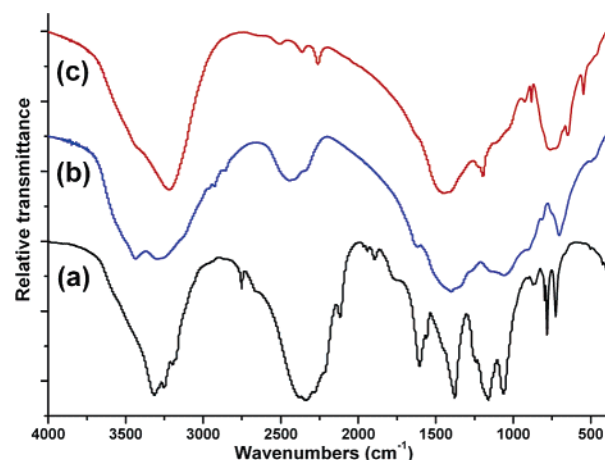observed in a narrow temperature range centered at 100 °C. Meanwhile, there is almost no mass loss at 180 °C for the mixed sample, whereas neat NH$_3$BH$_3$ loses weight up to a temperature of 200 °C. Thus, TG, DTG, and TPD measurements confirm that Ni$_{0.88}$Pt$_{0.12}$ catalysts result in an enhanced thermal decomposition of NH$_3$BH$_3$, with a lowered heating temperature and an increased rate of mass loss.

Two typical thermally decomposed samples, prepared by heating NH$_3$BH$_3$ with and without Ni$_{0.88}$Pt$_{0.12}$ catalysts at 120 °C for 2 h, have been characterized by IR, ICP, and XRD to analyze the composition of the thermolysis product. Figure 10 shows the FTIR spectra of unheated NH$_3$BH$_3$ and two thermally decomposed samples. The corresponding data of neat NH$_3$BH$_3$ (Figure 10a) agree well with reported results: the main absorbance bands centered at 3320−3200, 2335, 1605, 1377, 1160 (1063), and 797 (727) cm^{-1} are assigned to the modes of N−H stretching, B−H stretching, N−H bending, N−H out of plane, B−H torsion, and B−N stretching, respectively.[29] It can be seen from Figure 10b that the relative absorbance intensities of B−H stretching, B−H torsion, and N−H bending modes evidently decrease compared to the data of unheated NH$_3$BH$_3$, indicating the partial break of B−H and N−H bonds. In comparison, the corresponding B−H modes and N−H bending mode almost disappear in the spectrum of the thermally decomposed sample obtained with catalysts (Figure 10c). Therefore, Ni$_{0.88}$Pt$_{0.12}$ catalysts facilitate the dissociation of B−H and N−H bonds during the decomposition of NH$_3$BH$_3$. According to TG and FTIR measurements, we envisage that the catalyzed thermolysis of NH$_3$BH$_3$ leads to the formation of (BNH$_x$)$_n$ at 120 °C, along with the release of H$_2$ and other volatile boric compounds. ICP analysis of the obtained product confirms an elemental composition of B:N:H = 1:1:1.4. Furthermore, XRD patterns (Figure S5) indicate that the thermally decomposed product is a white noncrystalline solid, while NH$_3$BH$_3$ is crystalline.

From the above investigations, the as-synthesized Ni$_{1-x}$Pt$_x$ hollow spheres, especially Ni$_{0.88}$Pt$_{0.12}$ hollow spheres, exhibit

(29) Baumann, J.; Baitalow, F.; Wolf, G. *Thermochim. Acta* **2005**, *430*, 9.

favorable catalytic activities in both the hydrolysis and the thermolysis of NH_3BH_3. Some preliminary interpretations are suggested as follows to understand their catalytic performance. On one hand, the nest-like morphology and structure of the obtained $Ni_{1-x}Pt_x$ hollow spheres are beneficial factors for their high catalytic activities. Porous surfaces and submicrometer sizes endow the catalysts with high surface areas (e.g., 105 m^2 g^{-1} for $Ni_{0.88}Pt_{0.12}$) and large surface-to-volume atomic ratio, which are undoubtedly correlated with numerous catalytic sites. The open hollow structure may provide both the inner and the outer surfaces contact between catalysts and NH_3BH_3. Since the hydrolysis of NH_3BH_3 is determined to be a zero-order and heterogeneous reaction, the adsorption of NH_3BH_3 on the catalyst surface is an important process. Large quantities of active sites would thus result in enhanced kinetics. On the other hand, transition metals (Ir, Ru, and Rh) and their complexes have been demonstrated to be appropriate catalysts for the dehydrocoupling/dehydrogenation of amine borane or borane adducts with hydrogen elimination and B−N bond formation,[20,30] and transition metals such as Pt, Rh, and Pd can catalyze the hydrolysis of NH_3BH_3.[13] It is possible that the interaction between NH_3BH_3 and $Ni_{1-x}Pt_x$ promotes the hydrolysis and thermal decomposition of NH_3BH_3. Definite statements to the related catalytic mechanism as well as the structure of the reaction product have not been obtained in this work and hence still require further studies.

Conclusions

In summary, we have demonstrated the synthesis and catalytic study of submicrometer-sized $Ni_{1-x}Pt_x$ ($x = 0, 0.03$, 0.06, 0.09, and 0.12) hollow spheres. The obtained hollow spheres that have been prepared through a PSA-assisted template route exhibit favorable catalytic activities in the hydrolysis and thermolysis of ammonia borane with quick generation of hydrogen. The reaction system consisting of NH_3BH_3 and the nest-like $Ni_{1-x}Pt_x$ hollow spheres may find some possible applications in the field of small hydrogen fuel cells. Furthermore, the present synthesis route can be extended to prepare other alloy hollow spheres. The synthesized submicrometer-sized $Ni_{1-x}Pt_x$ hollow spheres might also be useful as catalysts for other reaction systems such as hydrogenation and oxygen reduction.

Supporting Information Available: Typical SEM and TEM images and EDX spectra of $Ni_{1-x}Pt_x$ ($x = 0.03, 0.06, 0.09$), SEM image of commercial Ni powders, hydrogen evolution graph, TPD curve, and XRD patterns. This material is available free of charge via the Internet at http://pubs.acs.org.

IC061712E

(30) (a) Jaska, C. A.; Temple, K.; Lough, A. J.; Manners, I. *Chem. Commun.* **2001**, 962. (b) Jaska, C. A.; Temple, K.; Lough, A. J.; Manners, I. *J. Am. Chem. Soc.* **2003**, *125*, 9424. (c) Jaska, C. A.; Manners, I. *J. Am. Chem. Soc.* **2004**, *126*, 9776.